

Relaxation Times for Magnetization Reversal in a High Coercivity Magnetic Thin Film

N. D. Rizzo,* T. J. Silva, and A. B. Kos

Electromagnetic Technology Division, National Institute of Standards and Technology, Boulder, Colorado 80303
(Received 17 March 1999)

We used a magneto-optical Kerr effect microscope to measure 180° magnetization reversal in a high coercivity $\text{CoCr}_{10}\text{Ta}_4$ thin film subjected to nanosecond field pulses. Exponential magnetization decay occurs for pulse duration $t_p < 10$ ns followed by logarithmic decay for $t_p > 10$ ns, indicating a crossover from nonequilibrium magnetization relaxation at short t_p to metastable equilibrium and thermal relaxation for longer t_p . We conclude that the nonequilibrium magnetization relaxation time (τ_n) and that the average relaxation time of microscopic thermal fluctuations (τ_0) is $\tau_n = \tau_0 \approx 5$ ns.

PACS numbers: 75.40.Gb, 75.50.Ss, 75.50.Vv

The time required for 180° magnetization reversal has recently received renewed interest primarily because of its relevance to the data storage industry [1,2]. A 180° magnetic reversal is initiated typically in one of two ways: either we apply a magnetic field so that the energy barrier to reversal remains finite and reversal occurs by thermally assisted hopping or we apply a large enough field so that reversal is energetically favored independent of thermal effects. In the latter case, the magnetic reversal proceeds with some nonequilibrium or “dynamic” relaxation time τ_n that has been measured to be on the order of nanoseconds or less in exchange coupled materials with uniform, uniaxial anisotropy [3–6]. Calculations using the Landau-Lifshitz-Gilbert (LLG) equation have yielded a value of τ_n in good agreement with the experimental results for the simple case of coherent rotation of the magnetization [4,6]. In the case of a finite energy barrier E_B , reversal occurs with the scaled relaxation time given by the Arrhenius-Néel law, $\tau_{\text{th}} = \tau_0 \exp(E_B/k_bT)$, where τ_0 is the average relaxation time in response to a thermal fluctuation [7]. Brown calculated τ_0 for a single-domain Stoner-Wohlfarth particle to be in the range $10 \text{ ps} < \tau_0 < 1 \text{ ns}$ [8], the exact magnitude depending upon several parameters, such as applied field H and magnetic damping constant α , which reflects the decay rate of coherent magnetic precession. Experimental determination of τ_0 has also been limited to simple systems, such as single-crystal Ni, that exhibit exponential magnetization decay (indicating a single energy barrier), in which case τ_0 was determined to be on the order of several nanoseconds [9].

For a more complex system containing a large number of interacting magnetic reversal volumes and a wide distribution of energy barriers—such as high coercivity magnetic recording media with weak exchange coupling and random anisotropy—the magnetic relaxation times (τ_n and τ_0) cannot be calculated analytically, but instead must be determined using complex micromagnetic simulations [10]. Experimental determination of these relaxation times for such complex systems have been ambiguous [11–13], in part because the broad distribution of energy barriers has prevented the clear separation of nonequilibrium reversal and thermally assisted reversal.

In this Letter, we report on the first unambiguous measurement of τ_n and τ_0 for a magnetic thin film containing a broad distribution of interacting energy barriers. We used a magneto-optical microscope to measure 180° magnetization reversal in a high coercivity $\text{CoCr}_{10}\text{Ta}_4$ magnetic film after exposing the film to nanosecond field pulses. We observed a magnetization response to step changes in H consisting of exponential decay for pulse duration $t_p < 10$ ns followed by logarithmic decay for $t_p > 10$ ns. This change in response indicates a crossover from nonequilibrium magnetization relaxation at short t_p , to metastable equilibrium and thermal relaxation for longer t_p . Therefore, the initial magnetization response is well described by nonequilibrium statistical mechanics, where exponential relaxation of macroscopic parameters is expected in a linear regime [14]. The nonequilibrium relaxation time was measured to be $\tau_n \approx 5$ ns in this linear regime before magnetic saturation occurs. We apply Onsager’s regression hypothesis [15] to conclude that the average magnetization relaxation time for microscopic thermal fluctuations is $\tau_0 = \tau_n \approx 5$ ns.

A coplanar waveguide was used to generate high magnetic fields of nanosecond duration. Uniform magnetic fields are produced directly above the center conductor of the waveguide when a current pulse passes through. The field magnitude scales inversely with center conductor width. For the measurements described here, the width was $10.6 \mu\text{m}$.

A $\text{CoCr}_{10}\text{Ta}_4$ film of thickness $\delta = 25$ nm along with a Cr underlayer of the same thickness was sputter deposited onto the region directly over the center conductor of the dielectric-coated coplanar waveguide. We measured a codeposited sample of the film using an alternating gradient magnetometer and determined the remanent magnetization to be $M_r = 490 \text{ kA/m}$ (490 emu/cm^3) and the remanent coercivity for a field pulse duration of 1 s to be $H_{\text{cr}}(1\text{s}) = 83 \text{ kA/m}$ (1040 Oe).

A high voltage pulse generator (200 V maximum) was used to send nanosecond current pulses (2–300 ns pulse duration) through the waveguide and produce in-plane magnetic field pulses as large as 150 kA/m (1875 Oe). The rise time and fall time of the pulse generator was

approximately 2 ns, so that a minimum pulse duration of approximately 2 ns was possible using FWHM as definition of pulse duration. The waveguide field was calculated assuming a uniform current density through the center conductor using the Biot-Savart law. The amplitude and duration of the waveguide pulse were recorded using a high speed oscilloscope.

The waveguide field pulse was combined with an external dc bias field provided by Helmholtz coils. The bias field made larger applied field amplitudes possible without risking damage to the waveguide and did not affect the measurement results [16]. The bias field amplitude was a constant 66 kA/m (825 Oe) for the duration of the waveguide pulse.

The switching caused by a given field pulse was quantified using a wide-field magneto-optical Kerr effect (MOKE) microscope which was optimized for detecting longitudinal MOKE at a wavelength of 545 nm. For each data point, the film was saturated in the positive x direction using the external Helmholtz coils. Then, a digital image of the remanent state of the film was acquired using a 16-bit CCD camera. Next, the dc bias field was applied and a current pulse was delivered to the waveguide, producing a field in the negative x direction. Finally, a second image of the film was acquired and electronically subtracted from the first image to obtain the relative change in magneto-optic contrast. This difference image was averaged over a $6 \mu\text{m} \times 120 \mu\text{m}$ area to determine the average change in the remanent magnetization of the film.

We examined the time dependence of the magnetization response in a fixed field. The results are shown in Fig. 1, where curves of remanent magnetization $M_r(t_p)$ for several values of H are plotted against pulse duration t_p with a logarithmic time axis. (We use H to designate the total field amplitude, which is the sum of the bias field and the pulse field.) For low fields, the magnetization appears to decrease logarithmically for increasing t_p . However, as the field increases, a kink in the magnetization response begins to appear at $t_p = 10$ ns. Finally, for the largest fields, saturation occurs for $t_p < 10$ ns, and the time required for saturation decreases with increasing field amplitude.

We verified that this kink is not an artifact of the 2 ns rise time of the pulse generator or of the use of FWHM in our definition of t_p : the kink was also observed using a 40 V pulse generator having a 500 ps rise time (see Fig. 1). We interpret the kink in our data as indicating a crossover in magnetization response at $t_p \approx 10$ ns.

For $t_p > 10$ ns, the magnetization decreases logarithmically with a maximum slope when $M_r(t_p) \approx 0$. Such behavior is characteristic of thermally assisted magnetization reversal for a system containing a distribution of energy barriers [17]. Furthermore, the logarithmic slope, $S_r \equiv dM_r(t_p)/d \log(t_p)$, is also proportional to the irreversible susceptibility, $\chi_{\text{irr}} \equiv dM_r(t_p)/dH$, where χ_{irr} was derived from the hysteresis curve for $t_p = 10$ ns

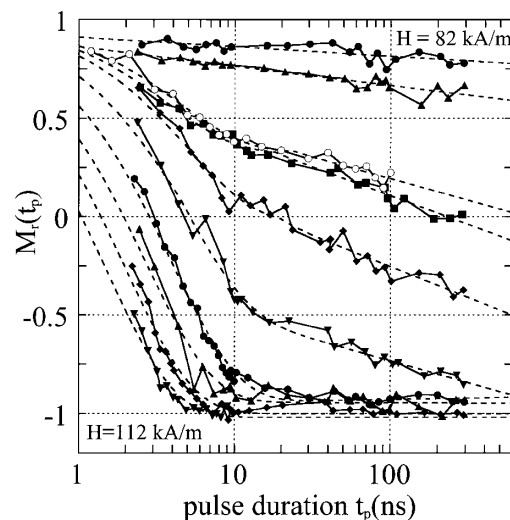


FIG. 1. Normalized remanent magnetization $M_r(t_p)$ of the $\text{CoCr}_{10}\text{Ta}_4$ thin film vs pulse duration t_p for field values $H = 82, 86, 90, 92, 94, 97, 102, 105, 108, 112$ kA/m. The data with open circles ($H = 90$ kA/m) were taken using a faster pulse generator with a 500 ps rise time. The dotted lines are fits of an exponential function for $t_p < 10$ ns and of a logarithmic function for $t_p > 10$ ns. The data for the two lowest fields are fit to a logarithmic function for all t_p .

(Fig. 2). Changes in χ_{irr} for $10 < t_p < 300$ ns were insignificant. This proportionality is a further signature of thermal relaxation [17,18]. The ratio of S_r to χ_{irr} can then be defined as the fluctuation field H_f , a fictitious field that is a measure of the thermal energy affecting the magnetization [18]. For $10 < t_p < 300$ ns, we find $H_f \approx 800$ A/m (10 Oe).

For $t_p < 10$ ns, the slope of the magnetization response is distinctly enhanced and does not decrease until either $t_p > 10$ ns or $M_r(t_p) \approx -M_r$, at which point the magnetization is saturated by the applied field pulse. This behavior is clear evidence for a crossover in magnetization response from metastable equilibrium with thermal relaxation for $t_p > 10$ ns, to nonequilibrium relaxation for shorter pulse duration: the magnetization requires approximately 10 ns to come into equilibrium with the applied field.

We fitted an exponential function to the data for $t_p < 10$ ns and a logarithmic function to the data for $t_p > 10$ ns. The data for the two lowest fields were fit to a logarithmic function over the entire range of t_p since there was no significant change in slope for $t_p < 10$ ns and $t_p > 10$ ns. The fitting results are also shown in Fig. 1. The reduced χ^2 of the fits ranged from 0.3 to 1.11, with the exception of the fit for $H = 105$ kA/m, which had $\chi^2 \approx 4$. The exponential fit gives a characteristic relaxation time τ for that particular applied field amplitude H in the nonequilibrium regime. The dependence of τ on H is shown in Fig. 3. The error bars designate 68% confidence limits and were derived using constant χ^2 boundaries [19]. The linear dependence of $1/\tau$ on $H > 100$ kA/m (1250 Oe) has

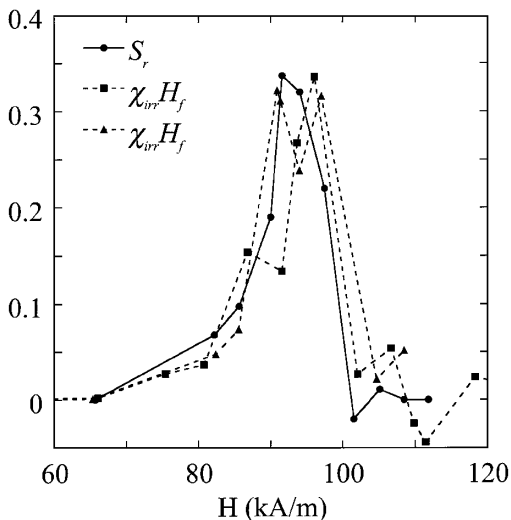


FIG. 2. Comparison between the logarithmic slope of magnetization response $S_r = dM_r(t_p)/d\log(t_p)$ for $10 < t_p < 300$ ns and the irreversible susceptibility $\chi_{irr} = dM_r(t_p)/dH$ for $t_p = 10$ ns, both normalized to M_r and plotted vs applied field H . Changes in χ_{irr} for $10 < t_p < 300$ ns were insignificant. Two separate measurements of χ_{irr} are shown and both have been multiplied by a constant $H_f = 800$ A/m (10 Oe), defined as the thermal fluctuation field.

also been observed for 180° magnetization reversal in high coercivity particular tape recording media [1,11] and even for low coercivity materials such as $\text{Ni}_{80}\text{Fe}_{20}$ [20]. The functional form fitted to the data is $\tau = S_w/(H - H_0)$, yielding a “switching speed” of $S_w = 29.7 \mu\text{s} \cdot \text{A} \cdot \text{m}^{-1}$ ($373 \text{ ns} \cdot \text{Oe}$). A flat line was fitted to the data for $H < 100$ kA/m (1250 Oe), yielding $\tau \approx 5$ ns. This low field behavior has not been reported before in switching speed studies of either hard or soft materials.

The exponential magnetization response to step changes in field, along with the large number of interactions in the film, strongly suggests that the macroscopic magnetization behavior is well described by nonequilibrium statistical mechanics. In this picture, the macroscopic magnetization relaxation time τ_n is a constant of the material in a linear response regime. The linearized equation of motion is then given by $dM/dt = -(M - M_a)/\tau_n$ [14], where M_a is the asymptotic value of the magnetization determined by H , so that exponential magnetization decay occurs with time constant $\tau = \tau_n$.

The decrease in τ at higher fields occurs because of the nonlinearity introduced by saturation. In fields large enough to cause saturation, the linear theory continues to predict exponential decay to some value of $M_a < -M_r$ that the system cannot reach. Saturation cuts off the exponential approach to M_a when $M = -M_r$, with the result that the fitted exponential relaxation time τ will be shorter than the relaxation time of the linear theory τ_n . If we take $M_a = M_r - \chi^{(1)}(H - H_0)$, where $\chi^{(1)}$ is the first coefficient in a Taylor series expansion of χ about $H = H_{cr}$, then one can show that in the nonlinear regime $\tau \approx (M_r \tau_n)/[\chi^{(1)}(H - H_0)]$. The full dependence of τ

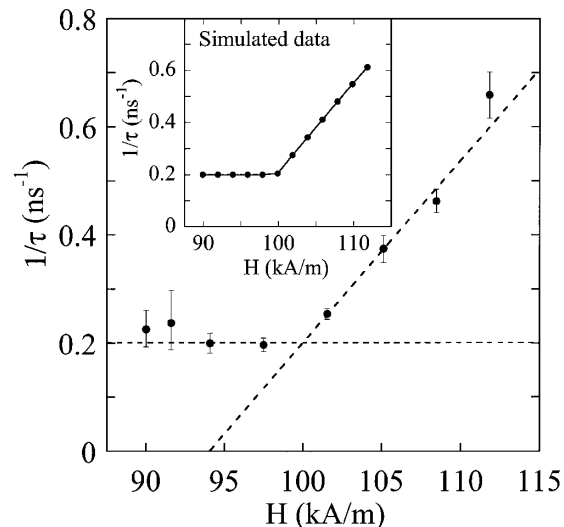


FIG. 3. Inverse relaxation time $1/\tau$ vs applied field H as determined from exponential fits to the magnetization response for $t_p < 10$ ns. For $H > 100$ kA/m (1250 Oe), the function $\tau = S_w/(H - H_0)$ is fitted to the data, yielding $S_w = 30 \mu\text{s} \cdot \text{A} \cdot \text{m}^{-1}$ ($373 \text{ ns} \cdot \text{Oe}$). For $H < 100$ kA/m, a straight line is fitted to the data, yielding $\tau \approx 5$ ns. Inset: $1/\tau$ vs H as determined by exponential fits to simulated data that was generated assuming exponential magnetization relaxation combined with saturation effects.

on H was also reproduced through a numerical simulation, where exponential functions were fit to magnetization decay data that was generated using the exponential relaxation of the linear theory and imposing the cutoff of decay at saturation (Fig. 3, inset).

Knowledge of the macroscopic nonequilibrium magnetization relaxation in a linear regime also gives information on the relaxation of microscopic thermal fluctuations while in equilibrium. Onsager’s regression hypothesis (ORH) (proven by the fluctuation-dissipation theorem [21]) states that, on average, the relaxation (or regression) of microscopic thermal fluctuations while in equilibrium must obey the same equations that govern the macroscopic relaxation of a nonequilibrium state toward equilibrium (in the limit of linear response) [15,22]. By simple application of ORH, we conclude that the average relaxation time in response to thermal fluctuations (τ_0) is the same as the magnetization relaxation time to equilibrium after an instantaneous change in H (τ_n). Therefore, we also conclude that $\tau_0 = \tau_n \approx 5$ ns. This result then explains the sharpness of the transition for $t_p < 10$ ns: faster reversal of M cannot occur, whether it is thermally assisted or dynamic in nature (due to H alone), insofar as linear response applies.

Effects such as an inverse dependence of τ on H and a transition from thermal to dynamic relaxation have been observed for more homogeneous, exchange-coupled magnetic systems where a single energy barrier description was appropriate [1,20,23]. Such phenomena were adequately explained in terms of viscous motion of domain walls. We have observed correlated regions of reversed

magnetization along the direction of H in our Kerr images, suggestive of domainlike structures. The correlation length has an approximate maximum at $M_r(t_p) = 0$ and decreases as saturation is approached, which suggests that the magnetization reverses by dipole-induced growth of the correlated regions along the direction of H [24].

We propose a microscopic picture of reversal by analogy to viscous domain wall motion to explain the observed macroscopic magnetization response. We assume that a reversed region nucleates and grows predominantly along the applied field direction until it collides with a pinning site in an average distance λ . The average equilibrium size of the reversed region depends linearly on applied field, or $\lambda = \chi_\lambda(H - H_0)$. The growth of the region occurs with a velocity $\nu = \mu(H - H_0)$, where μ is the growth mobility and H_0 is the nucleation field, by analogy with domain wall motion [25]. Exponential response is derived by assuming a random distribution of pinning sites, such that collision with a pinning site occurs with a probability per unit length $1/\lambda$, defining a Poisson point process of rate $1/\lambda$. The probability of a nucleated region expanding a distance x before being pinned when far from saturation is then $\exp(-x/\lambda)$, from which it can be shown that $M(t) = M_r[1 - (2\lambda/\lambda_s) + (2\lambda/\lambda_s)\exp(-\nu t/\lambda)]$, where λ_s is the value of λ at saturation and the factor of 2 results from growth in both the positive and negative field directions. Therefore, the exponential relaxation time $\tau = \lambda/\nu = \chi_\lambda/\mu$ is independent of H until saturation occurs. As H increases further, $\lambda = \lambda_s$, but ν continues to increase so that $\tau = \lambda_s/\nu = \lambda_s/\mu(H - H_0)$.

We estimate $\lambda_s \approx 1.4 \mu\text{m}$, derived from the average correlation length along the applied field direction for the Kerr images at $M_r(t_p) = 0$ and in the nonequilibrium regime ($t_p < 10$ ns). Using $S_w = \lambda_s/\mu$, we calculate $\mu = 0.047 \text{ m}^2 \cdot \text{s}^{-1} \cdot \text{A}^{-1}$ ($3.8 \text{ m} \cdot \text{s}^{-1} \cdot \text{Oe}^{-1}$), compared with $\mu = 0.2 \text{ m}^2 \cdot \text{s}^{-1} \cdot \text{A}^{-1}$ ($16 \text{ m} \cdot \text{s}^{-1} \cdot \text{Oe}^{-1}$), a value recently obtained with a NiFe alloy [20].

We can also estimate the damping constant α . The approximate reversal time for coherent spin rotation is $\tau_{\text{LLG}} \approx \alpha/\gamma\mu_0(H - H_0)$ [26]. The velocity of domain growth is then $\nu \approx a/\tau_{\text{LLG}} = a\gamma\mu_0(H - H_0)/\alpha$, where a is the domain wall width. Therefore, we have $\alpha \approx a\gamma\mu_0/\mu$ [27], where γ is the gyromagnetic ratio and μ_0 the permeability of free space. If we use the minimum length of a 180° magnetic transition as an estimate for $a \approx M_r\delta/2\pi H_{\text{cr}} \approx 20 \text{ nm}$ [28], we obtain $\alpha = 0.095$ compared with $\alpha \approx 0.02$, measured for single-crystal CoCrTa by ferromagnetic resonance [29].

In summary, we find that after a step change in H , the magnetization relaxes exponentially with a time constant $\tau_n \approx 5$ ns in a linear regime, which also implies (using ORH) that the average relaxation time for thermal fluctuations is $\tau_0 \approx 5$ ns. The statistical nature of the microscopic magnetization reversal results in the observed macroscopic exponential magnetization response. Microscopic reversal occurs through the nucleation, growth, and

random pinning of reversed regions of magnetization. The finite length of the reversed regions, coupled with their finite velocity of growth, results in a macroscopic reversal time (τ_n) that is proportional to, but much larger than, the microscopic reversal time (τ_{LLG}) given by LLG dynamics.

This work was supported by the NIST Advanced Technology Program.

*Email address: rizzo@boulder.nist.gov

- [1] W. D. Doyle, S. Stinnett, C. Dawson, and L. He, *J. Magn. Soc. Jpn.* **22**, 91 (1998).
- [2] K. B. Klaasen and J. C. L. van Peppen, *IEEE Trans. Magn.* **35**, 625 (1998).
- [3] W. Dietrich, W. E. Probestor, and P. Wolf, *IBM J. Res. Dev.* **4**, 189 (1960).
- [4] D. O. Smith and K. J. Harte, *J. Appl. Phys.* **33**, 1399 (1962).
- [5] M. R. Freeman, W. K. Hiebert, and A. Stankiewicz, *J. Appl. Phys.* **83**, 6217 (1998).
- [6] C. H. Back *et al.*, *Phys. Rev. Lett.* **81**, 3251 (1998).
- [7] L. Néel, *Ann. Geophys.* **5**, 99 (1949).
- [8] W. F. Brown, Jr., *Phys. Rev.* **130**, 1677 (1963).
- [9] W. Wernsdorfer *et al.*, *Phys. Rev. Lett.* **78**, 1791 (1997).
- [10] J. D. Hannay, R. W. Chantrell, and H. J. Richter, *J. Appl. Phys.* **85**, 5012 (1998).
- [11] R. F. M. Thornley, *IEEE Trans. Magn.* **11**, 1197 (1975).
- [12] S. M. Stinnett, W. D. Doyle, P. J. Flanders, and C. Dawson, *IEEE Trans. Magn.* **34**, 1828 (1998).
- [13] W. D. Doyle, L. Varga, L. He, and P. J. Flanders, *J. Appl. Phys.* **75**, 5547 (1994).
- [14] L. D. Landau and E. M. Lifshitz, *Statistical Physics*, Part 1 revised by E. M. Lifshitz and L. P. Pitaevskii (Pergamon Press, New York, 1980), 3rd ed., p. 360.
- [15] L. Onsager, *Phys. Rev.* **37**, 405 (1931); **38**, 2265 (1931).
- [16] Hysteresis curves for $t_p = 3.7$ ns were measured both with and without a bias field and showed no significant difference.
- [17] R. C. Street and J. C. Wooley, *Proc. Phys. Soc. London Sect. A* **62**, 562 (1949).
- [18] E. P. Wohlfarth, *J. Phys. F* **14**, L155 (1984).
- [19] W. H. Press, B. P. Flannery, S. A. Teukolsky, and W. T. Vetterling, *Numerical Recipes in C* (Cambridge University Press, Cambridge, 1988), p. 551.
- [20] R. H. Koch *et al.*, *Phys. Rev. Lett.* **81**, 4512 (1998).
- [21] H. B. Callen and T. A. Welton, *Phys. Rev.* **83**, 34 (1951).
- [22] D. Chandler, *Introduction to Modern Statistical Mechanics* (Oxford University Press, New York, 1987), Chap. 8.
- [23] A. Kirilyuk *et al.*, *J. Magn. Magn. Mater.* **171**, 45 (1997).
- [24] B. Walsh, S. Austvold, and R. Proksch, *J. Appl. Phys.* **84**, 5709 (1998).
- [25] C. Kittel and J. K. Galt, *Solid State Phys.* **3**, 439 (1956).
- [26] D. O. Smith, *J. Appl. Phys.* **29**, 264 (1958).
- [27] J. F. Dillon, Jr., in *Magnetism*, edited by G. T. Rado and H. Suhl (Academic Press, New York, 1963), Vol. 3, p. 415.
- [28] B. K. Middleton, in *Magnetic Recording Technology*, edited by C. D. Mee and E. D. Daniel (McGraw-Hill, New York, 1990), 2nd ed., p. 2.1.
- [29] N. Inaba *et al.*, *IEEE Trans. Magn.* **33**, 2989 (1997).